

Chemical state of Ti in sodium alanate doped with TiCl_3 using X-ray photoelectron spectroscopy

Aline Léon^{a,*}, D. Schild^b, M. Fichtner^a

^a Institut für Nanotechnologie, Forschungszentrum Karlsruhe GmbH, P.O. Box 36 40, 76021 Karlsruhe, Germany

^b Institut für Nukleare Entsorgung, Forschungszentrum Karlsruhe GmbH, P.O. Box 36 40, 76021 Karlsruhe, Germany

Received 16 July 2004; received in revised form 16 November 2004; accepted 22 November 2004

Available online 16 August 2005

Abstract

In this work, a study of the evolution of the chemical state of Ti in sodium alanate doped with 5 mol.% of TiCl_3 using X-ray photoelectron spectroscopy (XPS) is presented. Samples ball milled at 2, 30 and 60 min were investigated. XPS analysis indicates that the titanium is partially reduced to the metallic state after 2 min of ball milling and completely reduced after 30 min of ball milling. Further milling does not change the valence state of the titanium. Moreover, the atomic concentration of titanium at the surface is decreasing with increasing milling time. Depth profile and atomic concentration analysis show that the samples are contaminated at the surface only by oxygen and carbon. Furthermore, the concentration of titanium as well as of the metallic aluminum is increasing with the sputtering time. Finally, the reduction of TiCl_3 during the milling process explains that the theoretical capacity of 5.6 wt.% is never reached experimentally with doped sodium alanate.

© 2005 Published by Elsevier B.V.

Keywords: Hydrogen absorbing materials; Sodium alanate; Ti-based precursor; XPS

1. Introduction

Complex aluminum hydrides became particularly attractive for hydrogen storage, since it was shown that dehydrogenation and hydrogenation cycling was feasible by using appropriate catalysts [1]. However, a better understanding of the identity and the mechanism of the active catalyst may help to develop more effective catalysts and to modify appropriately the properties of the reversible decomposition reaction of metal-doped NaAlH_4 . That is why research on this fundamental aspect concerning the Ti catalyst is of valuable interest.

In our recent work, X-ray absorption spectroscopy was applied to investigate the evolution of the chemical state of Ti as well as the local structure around Ti atoms after ball milling and during two different defined stages of the absorption/desorption reaction in sodium alanate doped with 5 mol.% TiCl_3 [2]. XANES analysis indicated that during the ball milling the valence state of the Ti species is reduced

from Ti^{3+} to Ti^0 [2]. Further reaction due to the release or the absorption of hydrogen does not affect the chemical state obtained after ball milling. Moreover, once ball milled with the NaAlH_4 the local structure around the Ti is completely changed compared to the initial structure in pure TiCl_3 . EXAFS analysis shows that the Ti atoms are associated only with Ti as next neighbors in the ball milled state as well as during subsequent desorption and absorption of hydrogen. Furthermore, an increase of the particle size and an ordering of the local structure is seen to evolve with the desorption and the absorption of hydrogen.

These results lead to open questions concerning the time of the reduction process from Ti^{3+} to Ti^0 (at what point does the valence state change during the milling process?) and the location of Ti (does it stay dispersed at the surface or is it driven into the lattice?). In this work, using X-ray photoelectron spectroscopy we make an attempt to answer these questions.

Herein, we report on the chemical state as well as on the depth profile of the different elements in sodium alanate doped with 5 mol.% TiCl_3 and ball milled for 2, 30 and 60 min.

* Corresponding author. Tel.: +49 7247 82 6778; fax: +49 7247 82 6368.
E-mail address: A.Leon@int.fzk.de (A. Léon).

2. Experimental details

All sample preparations were done in an argon-filled glove box equipped with a recirculation system to keep the water and oxygen concentrations below 1 ppm. Chemical operations were performed on the bench under purified nitrogen using Schlenk tube techniques. Commercially available NaAlH_4 (Chemetall, Frankfurt) was purified by a Soxhlet extraction with THF as described elsewhere [3]. According to elemental analysis the purified NaAlH_4 contained 7.6 ± 0.1 wt.% H and 0.2 ± 0.1 wt.% C.

The samples doped with Ti-based catalyst were prepared using TiCl_3 (99.999%, Sigma–Aldrich). A silicon nitride vial containing balls made of the same material was filled with 285 mg of TiCl_3 (5 mol.%) and 2 g of purified sodium alanate and sealed. The ball to powder weight ratio was about 20:1. The milling was carried out in a Fritsch P6 planetary mixer/mill at 600 rpm for 2, 30 and 60 min. In the following, the samples are labeled (bm2), (bm30) and (bm60) for the samples ball milled 2, 30 and 60 min, respectively. For comparison, samples of pure NaAlH_4 and TiCl_3 were also investigated.

For XPS analysis, the powder samples were prepared on In-foil and mounted on the sample holder. By means of a transfer vessel, samples were transferred from the glove box into the XPS instrument without exposing them to air.

XPS measurements were carried out under an ultimate pressure of 7×10^{-8} Pa with a PHI 5600ci spectrometer (Physical Electronics) equipped with a hemispherical capacitor analyzer and a multi-channel detector. XPS spectra were recorded using Mg $K\alpha$ (1253.6 eV) or monochromatic Al $K\alpha$ (1486.6 eV) X-ray sources. High-resolution scans of elemental lines were recorded at 11.75 eV pass energy of the analyzer, which yields a full-width-at-half-maximum (FWHM) of the Ag $3d_{5/2}$ line of 0.85 and 0.62 eV respectively. The energy scale of the spectrometer was calibrated with the Cu $2p_{3/2}$, Ag $3d_{5/2}$ and Au $4f_{7/2}$ lines [4] of pure and Ar^+ sputter cleaned metal foils. The angle of emission (the angle between the analyzer direction and the sample surface normal) was 25° for all measurements except for depth profiling. In this work, the C 1s line of ubiquitous hydrocarbons was not used as reference as hydrocarbons may react at the surface leading to a change of the C 1s binding energy. Consequently, the Cl $2p_{3/2}$ line (binding energy of 200.7 eV) observed with the conducting samples (bm2), (bm2)AD and (bm60)AS was used as an internal reference line for the non-conducting samples. The spectrometer was calibrated in a way that the standard deviation of binding energies is within ± 0.1 eV for conductors and within ± 0.15 eV for non-conducting samples.

Atomic concentrations were calculated using peak areas of elemental lines after Shirley background subtraction and taking account the sensitivity factors, the asymmetry parameters as well as the measured analyzer transmission function. Curve fitting was performed using non-linear least-square

fitting technique on Gaussian–Lorentzian sum functions provided by PHI Multipak software.

XPS depth profiles were acquired by alternate ion beam sputtering (Ar^+ , 3 keV, current density $15.4 \mu\text{A}/\text{cm}^2$) followed by XPS acquisition of elemental lines. The angle between the normal of sample surface and the ion gun was 43° and the angle of emission for photoelectrons 60° . During sputtering the ion beam was rastered over an area of $3 \text{ mm} \times 3 \text{ mm}$ with Zalar rotation applied to the sample.

Absorption and desorption of hydrogen were carried out in a modified Sieverts apparatus. A more detailed description of the apparatus and the reactor used can be found elsewhere [3,5].

3. Results and discussion

3.1. XPS survey spectra and atomic concentration

During the acquisition we observed a surface charging with TiCl_3 and NaAlH_4 , whereas the sample (bm2) was conducting.

Fig. 1 represents the survey spectra of the sample (bm2). All elements composing the material can be detected including the Ti 2p line. The main contaminants are oxygen and carbon. The atomic concentrations of the different elements for each sample investigated are given in Table 1. The uncertainties in the concentrations are within $\pm 10\%$. One can see that with increasing milling time the atomic concentration of titanium and chlorine is decreasing at the surface while the concentration of Na, Al, O and C is increasing.

3.2. Pure NaAlH_4 and pure TiCl_3

For the pure sodium alanate, the Al 2p line is observed at 75.4 eV while the binding energy of the oxygen at the surface is at 532.7 eV. The difference between these two energies

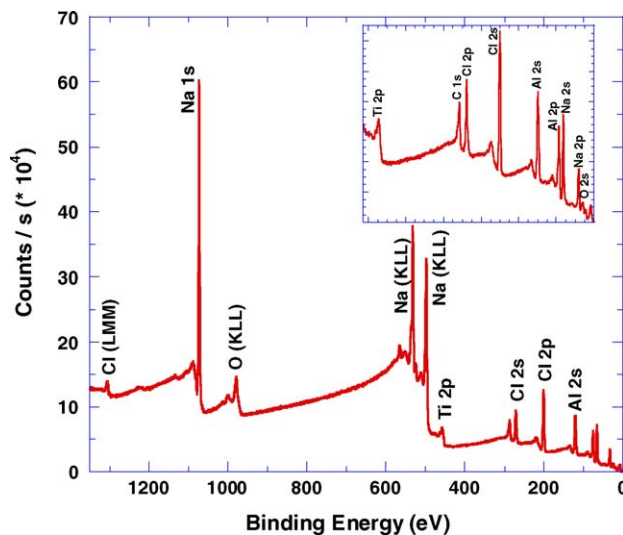


Fig. 1. XPS survey spectra of the sample (bm2). The inset is the magnification of the spectra at low binding energy (between 0 and 490 eV).

Table 1

Atomic concentrations obtained by the study of the survey surveys of NaAlH₄, TiCl₃ and ball milled NaAlH₄ doped with 5 mol.% of TiCl₃

Sample	Atomic concentration (%)							
	C	O	Na	Al	Al ³⁺	Al ⁰	Cl	Ti
NaAlH ₄	4.7	32.5	28.1	34.0			0.5	
TiCl ₃		8.4					65.9	25.7
(bm2)	7.3	32.8	24.9	21.5	18.1	3.4	10.6	2.8
(bm2) AD		6.9	16.4	60.3	21.6	38.7	11	5.3
(bm30)	8.4	35.7	25.4	24.7	20.1	4.6	5.3	0.6
(bm60) AD	9.9	34.6	25.5	25.4	21.1	4.3	4.1	0.5
(bm60) AD		7.5	17.5	63.1	19.8	43.3	7.8	4.2

AD: after depth profiling.

is equal to 457.3 eV, which is comparable to 457.3 eV of AlO(OH) but not to 456.6 eV of Al₂O₃ [4].

The Ti 2p spectrum of TiCl₃ is fitted well by one doublet, i.e. Ti 2p_{3/2} and Ti 2p_{1/2}. The Ti 2p_{3/2} line of TiCl₃ has a binding energy of 459.8 eV when referenced to the Cl 2p_{3/2} line at 200.7 eV. In a previous work, the reported binding energies of Ti 2p_{3/2} and Cl 2p_{3/2} in TiCl₃ [6] were 458.5 and 199.5 eV when it is charge referenced to C 1s at 284.8 eV. The difference in binding energies between Ti 2p_{3/2} and Cl 2p_{3/2} lines are 259.0 eV [6] and 259.1 eV (this work). This confirms that the sample is TiCl₃. As the reference binding energy of Ti 2p_{3/2} is 458.5 and 458.6 eV [6] for TiCl₃ and TiO₂, respectively, we concluded that the oxygen present at the surface of TiCl₃ was bound as TiO₂.

3.3. Samples (bm2), (bm30) and (bm60)

The binding energies of elemental lines obtained in this work and from references are presented in Table 2.

The evolution of the Ti 2p line with the milling time is also represented in Fig. 2. The comparison of the Ti 2p line of pure TiCl₃ with the one of samples (bm2), (bm30) and (bm60) shows that ball milling induces shoulders at the Ti 2p

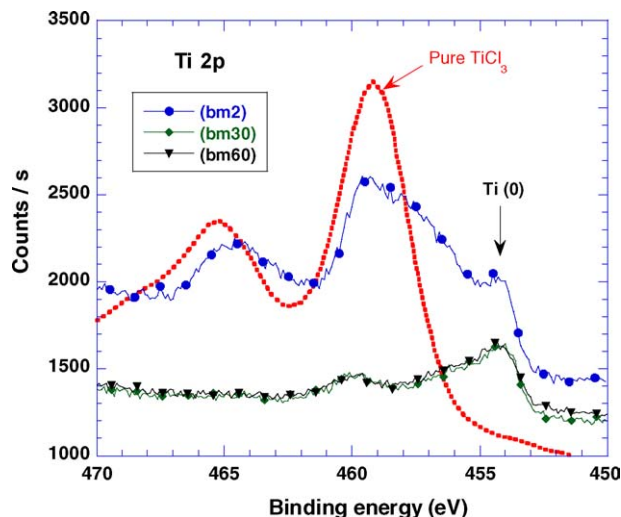


Fig. 2. Ti 2p spectra of pure TiCl₃ as well as of samples (bm2), (bm30) and (bm60).

line at low binding energies (i.e. 454.2 eV). We observed the same effect for the Al 2p line at 72.9 eV. These shoulders can be assigned to the metallic state of titanium and aluminium, as the reference energies for those states are 454.1 and 72.9 eV for Ti (0) and Al (0), respectively [4]. This result is in agreement with the result obtained using XAS spectroscopy concerning the shift of the valence state of Ti from (+3) to (0) during the milling process [2]. Moreover, the comparison of the Ti 2p line between the three samples shows that the Ti is partly reduced to the metallic state already after 2 min of ball milling (binding energies in that case are lying between the initial TiCl₃ and Ti⁰) while it is completely reduced to the zero-valence state after 30 min of ball milling. The titanium remains in this state with increasing milling time.

Concerning the non-metallic part of Al it can be observed that the binding energy of the Al 2p line is decreased from 75.4 eV (initial NaAlH₄ sample) to 75.2 eV after ball milling.

Table 2

Binding energies of elemental lines charged referenced to Cl 2p_{3/2} at 200.7 eV (this work)

Sample	Na 1s	Ti 2p _{3/2}	O 1s	C 1s	Cl 2p _{3/2}	Al 2p	Na 2s	Ref.
Al ^a						72.9		[4]
Al ₂ O ₃			531.0			74.4		[4]
AlO(OH)			531.5			74.2		[4]
Ti ^a		454.0						[6]
TiO ₂		458.6	529.8					[6]
TiCl ₃		458.5			199.5			[6]
TiCl ₃		459.8			200.7			This work
TiAl ₃ ^a		453.8				72.4		This work
NaAlH ₄	1073.9		532.7 , 534.2	^b	200.7	75.4	65.6	This work
(bm2) ^a	1073.7	454.2, 459.4	531.9 , 533.4	287.0 , 290.8	200.7	72.9, 75.2	65.5	This work
(bm30)	1073.6	454.2	531.9 , 533.4	287.0 , 290.8	200.7	72.8, 75.1	65.3	This work
(bm60)	1073.6	454.2	532.0 , 533.4	287.0 , 290.7	200.7	72.9, 75.1	65.3	This work
(bm2) AD ^a	1072.3, 1073.9	454.0	531.9 , 533.0		200.7	72.8 , 74.6	64.1 , 65.6	This work
(bm60)AD ^a	1072.3, 1073.9	454.0	532.0 , 533.3		200.7	72.8 , 74.8	64.0, 65.5	This work

Reference values charged referenced to C 1s are also given. Binding energies printed in bold are the most intense lines if several values are given.

^a Conducting samples.

^b C 1s line superimposed with the plasmon loss line of Cl 2s.

The difference in the binding energy between the most intense O 1s line at 531.9 eV and the Al 2p line of (bm2) assigned to the non-metallic state is equal to 456.7 eV. This value is comparable to the binding energy difference observed for Al₂O₃ [4].

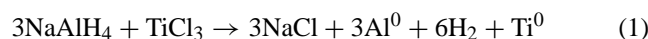
The ball milling shifts the Na 1s and Na 2s line by 0.3 eV to lower binding energy. This together with the decrease of the binding energy of Al 2p line after ball milling indicates an enhanced electron density within the alanate induced by the presence of metallic Ti and Al (i.e. by the introduction of the Ti-based precursor).

3.3.1. XPS depth profile

In the low binding energy region it can be observed that the conducting band and the Fermi edge are much more pronounced after sputtering, indicating that the sputtering process itself induces changes, i.e. a reduction of the samples. Fig. 3a represents the depth profile of sample (bm2) and (bm60). One can see that once the reacted surface layer has been removed, the atomic concentration of all the elements vary in a different manner. The Al signal steadily increases and the O signal decreases during sputtering. The Ti signal, Fig. 3b, shows a behaviour which depends on the milling time of the sample: an initial increase can be observed with the (bm2) sample which is followed by a subsequent decrease whereas a steady increase can be observed with the (bm60) sample. This is in accordance with SNMS depth profiles, which were obtained with similarly prepared samples [7]. The atomic concentration obtained after sputtering, Table 1, indicates that the amount of Ti, Cl and Al is increasing while the amount of Na and oxygen is decreasing. The surface seems then to be covered by NaCl and Al₂O₃. We also note that the contamination by carbon is only a surface effect.

High-resolution scans of elemental lines acquired directly after depth profiling show similar spectra for the two samples. After sputtering there is no alteration of the Cl 2p signal whereas the Na 1s line shows two components with a difference of about 1.6 eV in the binding energies. Moreover, curve fits to Al 2p spectra show that about 60% of Al is present in the metallic state whereas all the Ti is in the zero-valence state within the detection limit of the method.

From the XPS and XAS analysis [2], we can state that a certain molar fraction of the initial charge of sodium alanate reacts with the TiCl₃ during the milling process according to the following reaction:



When the sodium alanate is doped with 5 mol.% of TiCl₃, 15 mol.% of the initial sodium alanate is drawn off for the reduction of TiCl₃. The calculated value (according to Eq. (1)) of the hydrogen storage capacity for different concentration of the precursor and the measured value are shown in Table 3. One can see that after the first cycle the experimental and the calculated value are in agreement. Thus, the fact that the theoretical capacity of 5.6 wt.% is never

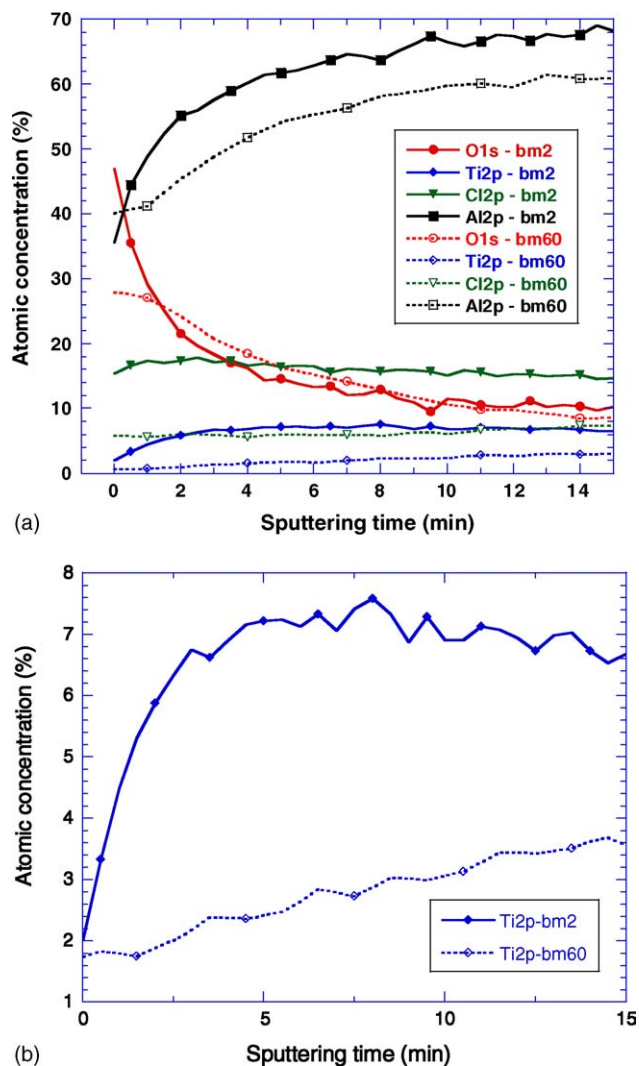


Fig. 3. (a) The XPS depth profiles of samples (bm2) and (bm60). (b) The magnification of the Ti 2p-bm2 and Ti 2p-bm60 XPS depth profiles.

reached experimentally with doped sodium alanate (which was also observed in [8]) is explained by the reduction of TiCl₃, which is taking place during the milling process.

In Eq. (1) there are three reduced Al atoms for one Ti atom, which give the stoichiometry of TiAl₃. Moreover, in the literature several studies assumed the formation of the TiAl₃ alloy [1,9–11]. However, it should be noted that even though it is possible to check the presence or the absence of TiAl₃

Table 3

Calculated and measured value of the hydrogen storage capacity after the first cycle according to Eq. (1) for sodium alanate doped with different concentrations of TiCl₃

TiCl ₃ (mol.%)	H ₂ (wt.%)	
	Calculated	Measured
0	5.6	5.6
2	5.2	5.1
4	4.9	5.0
5	4.7	4.65

at the surface with XPS, the experimental conditions in this study (milling vial, milling time, number of cycles, etc., . . .) is different from the previous ones. Knowledge of the atomic concentrations or the binding energies of elemental lines of Ti 2p_{3/2} and Al 2p lines allows to state about a possible alloying effect between Al and Ti at the surface. Table 2 reveals that the binding energy of the elemental lines of the (bm) samples without sputtering is not comparable to TiAl₃. Moreover, the atomic concentrations (cf. Table 1) of Ti and Al⁰ are similar for the (bm2) sample but not at the stoichiometric ratio of 1 to 3. Additionally, the increase of the milling time reduces the concentration of Ti at the surface and then do not match the TiAl₃ stoichiometry. From the present data one can conclude that TiAl₃ is not present at the surface but we cannot strictly confirm or exclude the presence of TiAl₃ in the bulk by XPS.

4. Conclusion

In the present study, it has been shown that there is a reduction of the valence state of TiCl₃ from (3+) to (0) within the first 2 min of ball milling. A complete reduction is observed after 30 min and this state remains with increasing milling time. Correspondingly, some of the Al in the sample is reduced to the metallic state. Moreover, with increasing milling time, the atomic concentration of titanium at the surface is decreasing while the concentration of metallic aluminium is increasing. XPS depth profiling shows that the contamination

of the samples by oxygen is only a surface effect. Spectra obtained after sputtering also indicates a surface contamination by carbon, which could be due to residual amounts of solvent in the alanate. Furthermore, depth profiles indicate more titanium and aluminum in the bulk than at the surface.

References

- [1] B. Bogdanovic, M. Schwickardi, *J. Alloys Compd.* 253–254 (1997) 1.
- [2] A. Léon, O. Kircher, J. Rothe, M. Fichtner, *J. Phys. Chem. B* 108 (2004) 16372.
- [3] M. Fichtner, O. Fuhr, O. Kircher, J. Rothe, *Nanotechnology* 14 (2003) 778.
- [4] J.F. Moulder, W.F. Stickle, P.E. Sobol, K.D. Bomben, J. Chastain (Eds.), *Handbook of X-ray Photoelectron Spectroscopy*, Perkin-Elmer Corporation, Physical Electronics Division, Eden Prairie, Minnesota, 1992.
- [5] O. Kircher, M. Fichtner, *J. Appl. Phys.* 95 (2004) 7748.
- [6] Ch. Sleigh, A.P. Pijpers, A. Jaspers, B. Coussens, R.J. Meier, *J. Electron Spectrosc. Relat. Phenom.* 77 (1996) 41–57.
- [7] M. Fichtner, P. Canton, O. Kircher, A. Léon, *J. Alloys Compd.* 404–406 (2005) 732–737.
- [8] G. Sandrock, K. Gross, G. Thomas, *J. Alloys Compd.* 339 (2002) 299.
- [9] C. Weidenthaler, A. Pommerin, M. Felderhoff, B. Bogdanovic, F. Schüth, *Phys. Chem. Chem. Phys.* 5 (2003) 5149.
- [10] M. Felderhoff, K. Klementiev, W. Grünert, B. Spiethoff, B. Tesche, J.M. Bellosta von Colbe, B. Bogdanovic, M. Härtel, A. Pommerin, F. Schüth, C. Weidenthaler, *Phys. Chem. Chem. Phys.* 6 (2004) 4369.
- [11] J. Graetz, J.J. Reilly, J. Johnson, A. Yu. Ignatov, T.A. Tyson, *Appl. Phys. Lett.* 85 (2004) 500.